PHYSICAL REVIEW B **91**, 140408(R) (2015)

Strong coupling between $P1$ diamond impurity centers and a three-dimensional lumped photonic microwave cavity

Daniel L. Creedon,[1] Jean-Michel Le Floch,[1] Maxim Goryachev,[1] Warrick G. Farr,[1]
Stefania Castelletto,[2] and Michael E. Tobar[1,*]

[1]*ARC Centre of Excellence for Engineered Quantum Systems, School of Physics, University of Western Australia, 35 Stirling Highway, Crawley, Western Australia 6009, Australia*

[2]*School of Aerospace, Mechanical and Manufacturing Engineering, RMIT University, Melbourne, Victoria 3000, Australia*

(Received 11 December 2014; revised manuscript received 1 February 2015; published 24 April 2015)

We report strong coupling between an ensemble of N impurity ($P1$) centers in diamond and microwave photons using a unique double-post reentrant cavity. The cavity is designed so that the magnetic component of the cavity field is spatially separated from the electric component and focused into the small volume in which the diamond sample is mounted. The novelty of the structure simultaneously allows the high magnetic filling factor (38.4%) and low frequencies necessary to interact, at low magnetic field, with transitions in diamond such as those in negatively charged nitrogen-vacancy and $P1$ centers. Coupling strength (or normal-mode splitting) of 51.42 MHz was achieved with $P1$ centers at 6.18 GHz and 220 mT in a centimeter-scale cavity, with a corresponding cooperativity factor of 4.7. This technique offers an alternative way, with some significant advantages, to couple 3D cavities to transitions in diamond and achieve the strong coupling necessary for applications to quantum information processing.

DOI: 10.1103/PhysRevB.91.140408 PACS number(s): 76.30.Mi, 42.50.Pq, 84.40.Fe, 31.30.Gs

Quantum systems that consist of spin ensembles coupled to a cavity mode are attracting attention as a promising physical realization for processing and storage of quantum information and for the realization of ultrasensitive high-resolution magnetometers [1] or to improve conventional electron-spin-resonance sensitivity [2]. A large ensemble of spins can allow collective coupling to the cavity modes, enabling the strong-coupling regime to be reached [3], the case in which the coupling strength between a photonic cavity mode and a spin ensemble exceeds the average linewidth of these two resonances. Whereas the coupling strength to individual spin is small, the collective coupling strength g_c is enhanced with a characteristic scaling factor of $\sqrt{N}$, where N is the number of identical spins in the interaction volume.

The spin ensemble can be used to store quantum information if strongly coupled to the cavity modes, which can then be used as a reliable readout system. Different types of spin ensembles have been studied for this purpose [4–6], with recent focus (due to scalability) on solid-state systems such as color centers in diamond [4,7,8] and rare-earth spin ensembles [9,10]. For the cavity subsystem, three-dimensional cavities in particular show great promise. In the case of transmon qubits, coupling to a three-dimensional (3D) cavity has enabled qubit decoherence to be suppressed when compared to two-dimensional (2D) strip-line resonators [11]. Strong coupling has also been achieved between an electron-spin ensemble and a 3D microwave cavity at room temperature [12] and between spin ensembles and several other systems [5,13]. Strong coupling of nitrogen-vacancy defects in diamond to strip-line resonators [4] is particularly interesting, as nitrogen is one of the most common impurities in diamond. Impurity spins and defect centers in diamond [14] have recently played a significant role because of their potential application as qubits in the field of quantum information, computing, and control. One of the most well studied defects in diamond is the nitrogen vacancy (NV) defect due to its extremely long electron-spin coherence time, approaching 1 s at 77 K [15]. The electron spin ($S = 1$) of the negatively charged defect (NV^-) can be read out optically via a "flying" qubit and can be coupled to nearby ^{13}C nuclear spins. Coupling to other paramagnetic impurities in close proximity can also be achieved, such as the $P1$ impurity of diamond ($S = 1/2$), commonly referred to as the C impurity, a substitutional replacement of a carbon atom in the lattice with a nitrogen atom, most commonly ^{14}N. Such cavity coupling to nearby NV dark spins is relevant for quantum information and sensing [16,17], and defects in diamond whose electron or nuclear spin state in ensemble could be coherently read out can offer a large space for implementing coherent quantum control of their spin or for use as a quantum memory. Here, we demonstrate operation in the strong-coupling regime for an ensemble of $P1$ impurities in diamond coupled to a 3D photonic cavity mode at microwave frequencies.

Measurements were performed on two diamond crystals (herein referred to as sample 1 and sample 2). The diamonds are high-pressure, high-temperature Sumitomo type-Ib bulk diamonds that are top and bottom surface cleaved along ⟨100⟩ faces and irradiated with 2 MeV electrons to a fluence of $1.11 \times 10^{18}/\text{cm}^2$ at $T < 80\,^\circ\text{C}$ to create vacancies and then annealed in vacuum at 900 °C for 2 h to form the NV centers. Independent electron paramagnetic resonance spectra of the diamonds taken after electron irradiation and annealing show clearly the $P1$ center region arising from substitutional N atoms and the NV center. The nitrogen ($P1$) concentration was determined to be 8.2–10 ppm, while the NV concentration was 3.1 ppm. The samples, each with dimensions $3.66 \times 3.66 \times 1.72$ mm, were cleaned in nitric acid and measured separately after being mounted at the center of the dual-post reentrant cavity, shown in Fig. 1. The principle of operation of a similar cavity was described in detail previously to couple magnons in an yttrium iron garnet (YIG) sphere near 20 GHz [18]. In this case we illustrate the

*michael.tobar@uwa.edu.au

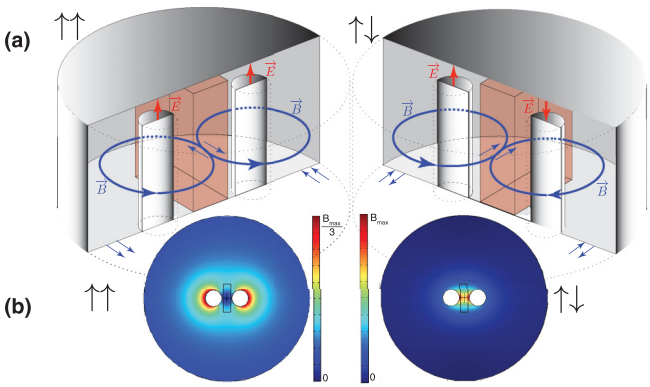

FIG. 1. (Color online) The field-focusing reentrant cavity used for the experiment. The shaded block between the posts is the diamond crystal. (a) A 3D cross section of the cavity operating in the dark mode (left) and bright mode (right). (b) The magnetic field density for the dark (left) and bright (right) modes in the plane at the center of the cavity height.

versatility of the cavity by designing the dark and bright modes in the lower gigahertz range relevant for coupling to spins in diamond. The cylindrical volume of the cavity contains two cylindrical posts with a height several tens of microns less than the height of the cavity. The dc magnetic field is applied in the $\langle 100 \rangle$ direction, therefore forming a $\theta = 55^\circ$ angle with the four possible orientations of NV and $P1$ along the $\langle 111 \rangle$ crystallographic axes.

The two lowest-order modes which may be excited in this cavity configuration are the so-called dark mode (DM) at 4.28 GHz and the bright mode (BM) at 6.18 GHz. The DM has a symmetric electric field component in the pair of reentrant cavity post gaps, which leads to cancellation of the magnetic field component at the center of the cavity due to the resulting antiparallel magnetic field contribution from each post. Thus, operation in the DM leads to a low magnetic field filling factor; that is, the fraction of magnetic field energy inside the volume of the diamond sample is low compared to the total volume of the magnetic energy in the cavity.

Conversely, the electric field of the BM is antisymmetric in the post gaps, which leads to enhancement of the magnetic field between the posts and a subsequently large magnetic field filling factor in the volume of the crystal. This type of cavity, a so-called multiple-post reentrant cavity [19,20], allows a large magnetic filling factor to be achieved in very small samples, something that would ordinarily require the use of a very small cavity with correspondingly (and usually undesirably) high eigenfrequencies. In the present work, given the dimensions of the diamond, cavity, and gap spacing used, we compute magnetic filling factors of 38.4% and 2.1% for the BM and DM, respectively [18].

The measurement technique employed in this work is similar to that in previous works investigating spins in solids at low temperatures using dielectric [21–24] and metallic cavities [18]. This approach has been used previously in whispering-gallery-mode resonators based on crystals with low dielectric loss, as the corresponding high Q factor and the existence of numerous closely spaced high-order modes allows them to act as sensitive antennae for the detection of tuned electron spin resonances. Whispering-gallery-mode techniques have also been used previously for the characterization of polycrystalline diamond [25]. In the case of whispering-gallery-mode resonators, the large population of many dozens of modes allows spin resonances to be tracked over a wide frequency range spanning several tens of gigahertz. However, in the present work it is more critical to achieve the highest magnetic filling factor in the diamond volume, and as such the accessible frequency span is closely centered around the bright-mode eigenfrequency. Although higher-order reentrant cavity modes exist, the lowest-order BM has the highest magnetic filling factor inside the diamond samples, and as such only this mode is monitored in the present work.

We consider the following Hamiltonian describing the interaction of NV^- spin and the $P1$ electron and nuclear spin with a magnetic field [17,26–29]:

$$H = D\left[\left(S_z^{\mathrm{NV}}\right)^2 - \tfrac{1}{3}(S^{\mathrm{NV}})^2\right] + (S^{\mathrm{NV}} \cdot J \cdot S^N) + (S^N \cdot A \cdot I^N) \tag{1}$$

where S^{NV} is the electron spin-1 operator of NV with z, the NV/$P1$-axis direction (along four equivalent diamond $\langle 111 \rangle$ axes); S^N is the nitrogen electron spin-$\frac{1}{2}$ operator; and I^N is the nitrogen nuclear spin-1 operator of the $P1$ center. The zero-field splitting of the NV electronic triplet is given by $D = 2.88$ GHz, and J and A are the fine-structure and hyperfine tensors, respectively, with $A/2\pi =$ [81.33,81.33,114.03] MHz. The last terms describe the $P1$ center, a nitrogen atom with an extra almost-free electron interacting with the N nuclear spin and with the electronic spin of the NV^- color center.

Several measurements were taken of the diamond samples in different orientations. Sample 1 was measured in two orientations, with the second being a rotation of 90° around the z axis of the crystal. The rotation had a minimal effect on the interactions observed, and as such sample 2 was measured in only one orientation. Using the spectroscopic technique described previously, the cavity dark mode at 4.28 GHz and the bright mode at 6.18 GHz were examined using a vector network analyzer while incrementally stepping the applied dc magnetic field. To check for power dependence, the input power to the cavity was swept over a range of 35 dB with no discernible effect other than a change in the signal-to-noise ratio of the measurement. Three regions of interaction were experimentally observed in the crystal. The cavity BM is seen to interact with NV^- impurities in the diamond sample over a region of applied magnetic field near 90 mT [see Figs. 2(a) and 2(b)], as well as $P1$ centers near 210–230 mT (see Fig. 3), whereas the cavity DM interacts with the $P1$ centers at approximately 120 mT.

Figure 2(a) shows the transmission spectrum of sample 1 as the applied magnetic field is swept and the transition frequency of the NV^- impurity is tuned into resonance with the cavity BM, resulting in an avoided frequency crossing for an applied field near 93 mT. Figure 2(b) tracks the frequency at the minimum transmission coefficient over this range of field in order to determine the slope of the interaction. This slope is extrapolated to find the zero-field splitting in Fig. 2(c), which, assuming a constant slope, was determined to be 2.87 GHz. Figure 2(c) also shows the higher-field interactions of the

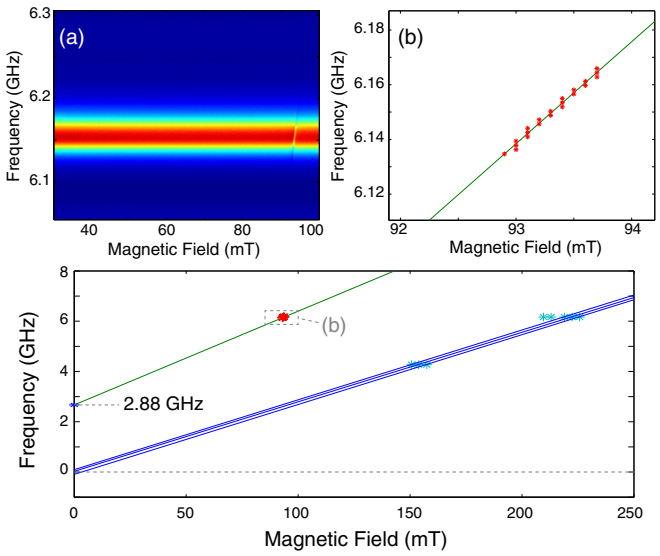

FIG. 2. (Color online) (a) Transmission spectrum of the "low-field" interaction where the NV^- transition between the $m_S = 0$ and $m_S = +1$ states is tuned across the cavity BM near 93 mT. (b) Frequency at the point of minimum transmission through the cavity over the range of the NV interaction. The slope of the line confirms the well-known zero-field splitting of ~2.87 GHz for this defect. (c) Large span plot incorporating (b) as well as showing interactions between nuclear hyperfine transitions of $P1$ centers and the cavity BM and DM.

dark mode near 120 mT and the bright mode near 220 mT. We attribute these interactions to the spin-flip transitions for $P1$ defects that conserve the nuclear spin of ^{14}N, where $m_I = -1,0,1$. From the data, we calculate a Landé g factor of 2.6 for the low-field NV^- interaction [Fig. 2(b)] and an approximate Landé g factor of 1.98 for the spin-flip transitions (labeled C–E in Fig. 3).

Figure 3 shows the transmission spectrum of the cavity BM when loaded with two different diamond samples. The nuclear spin of the $P1$ defect (most commonly, ^{14}N is $I = 1$) leads to an energy-level splitting into $2I + 1 = 3$ energy levels. This hyperfine spectrum of the $P1$ centers is clearly visible as three avoided crossings that correspond to the allowed nuclear-spin-conserving electronic transitions (i.e., the spin-flip transitions $m_S = \pm\frac{1}{2}$, $m_I = -1,0,+1$ levels, labeled C–E respectively). Also faintly visible for both samples is a set of two weaker interactions (indicated with arrows) in the interaction with the bright mode. This may be attributed to anisotropy in the hyperfine coupling caused by a geometrical Jahn-Teller distortion of the bond between the $P1$ center nitrogen atom and a neighboring carbon atom. The distortion is randomly oriented along one of the four ⟨111⟩ crystallographic directions, and the hyperfine splitting is determined by the angle between this distorted bond direction and the applied external magnetic field. When the applied field is parallel to the ⟨100⟩ crystallographic direction of the diamond, all of the carbon bond angles relative to the field are equivalent, so only three hyperfine lines are seen [5]. However, when the field is applied along the crystallographic ⟨111⟩ direction, a set of five lines is observed in the spectrum [16,30,31]. Thus, we attribute the detection of these weak transitions to a small misalignment of the crystallographic axes of the sample within the field or some internal strain of the crystal. Only the strongest three transitions are observed to interact with the dark mode due to its low magnetic filling factor and corresponding reduced sensitivity.

The hyperfine structure of $P1$ centers in diamond has been observed previously by coupling to superconducting transmission line cavities [5]. Here we demonstrate that the strong-coupling regime can be achieved between $P1$ impurity centers in diamond and photons in a 3D reentrant cavity due to the strong enhancement in magnetic filling factor. Figure 4 shows two slices through the transmission spectrum of the cavity BM when loaded with sample 1 shown in Fig. 3(a). The first slice at an applied field of 200 mT shows the normal transmission curve of the cavity bright mode far from the interaction, i.e., the bare mode centered at 6.198 GHz. In this case, the Q factor of the cavity mode is approximately $Q_L = 150$ when loaded with the diamond sample. The second curve shows the mode splitting when the $(m_s = \pm\frac{1}{2}, m_I = -1)$ transition of the $P1$ defect is tuned into resonance with the cavity at 220.5 mT, a splitting which is well modeled by a pair of coupled oscillators. We observe normal mode splitting

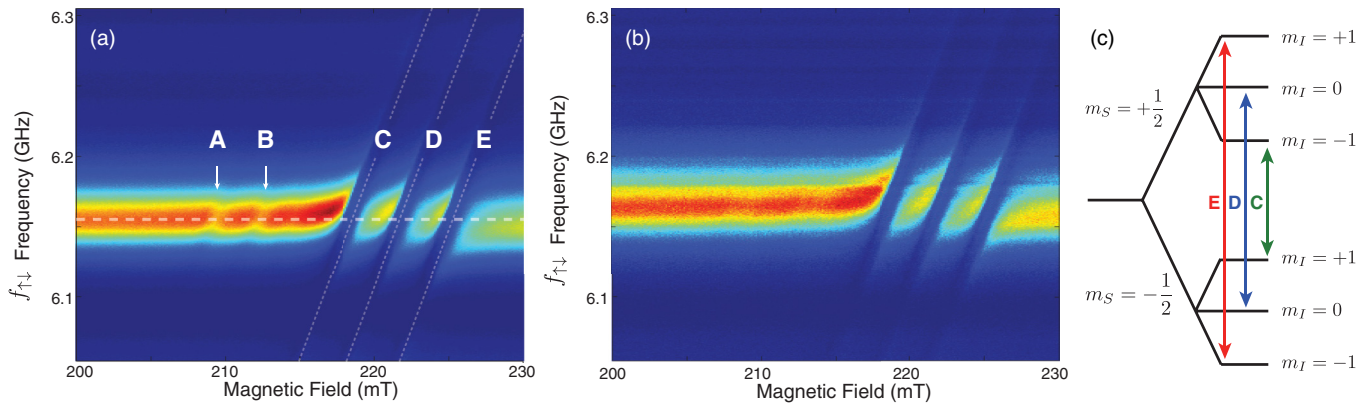

FIG. 3. (Color online) Transmission spectrum of the cavity near the bright mode with (a) sample 1 and (b) sample 2. The normal behavior of the cavity bright mode (i.e., no magnetic field dependence) is indicated in (a) as a horizontal dashed line. Three clear avoided crossings are visible (labeled C, D, and E), corresponding to the electron-spin transitions of the $P1$ centers that conserve the ^{14}N nuclear spin, as well as two weaker interactions (A and B) indicated by arrows. (c) The energy-level structure of the $P1$ center.

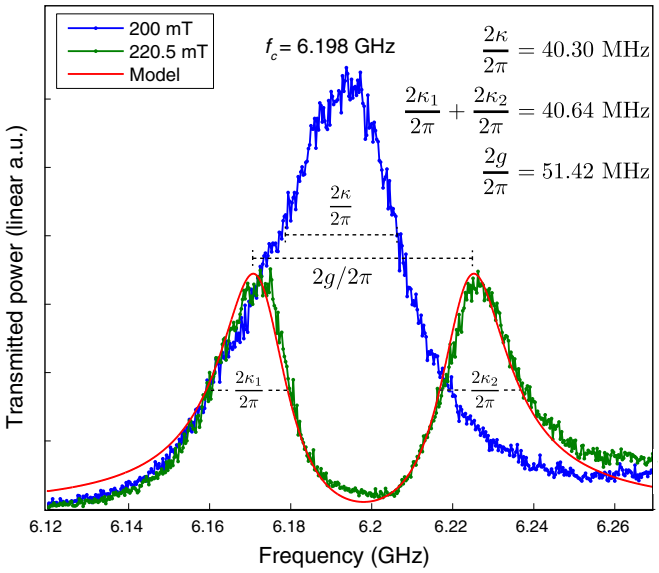

FIG. 4. (Color online) Demonstration of strong coupling between diamond $P1$ energy levels in sample 1 and the bright cavity mode. Slices through Fig. 3(a) at 220 and 220.5 mT are shown. The slices show the BM far from the interaction, as well as on resonance, where it interacts with the spin-flip transition labeled C in Fig. 3. The data are well modeled by a pair of coupled oscillators. The plot shows the largest ratio of splitting to linewidth achieved.

of $\Delta = 2g/2\pi = 51.42$ MHz, with the sum of the split-mode linewidths $2\kappa_1/2\pi$ and $2\kappa_2/2\pi$ equal to 40.64 MHz, i.e., a ratio of 1.3. We compute from the data that the density of coupled spins is approximately $1.6 \times 10^6/\mu\text{m}^3$ and deduce from the fit a dipolar spin broadening of $2\Gamma/2\pi \sim 13.6$ MHz. Thus, we calculate a cooperativity factor $C = g^2/\kappa\Gamma$ of 4.7, exceeding that measured by Schuster *et al.* [5] by nearly a factor of 3. We estimate that this is comparable to the cooperativity achieved by Ranjan *et al.* using a superconducting resonator [6].

In summary, strong coupling has been demonstrated between the nuclear spin of $P1$ impurity centers in diamond and the bright mode of a reentrant magnetic-field-focusing 3D cavity [18]. This result represents an improvement on the strong-coupling condition compared to previous work with planar superconducting cavities. In addition, we observed the NV^- electron-spin transition and the $P1$ spin-flip transition using the dark mode of the cavity, with comparatively low magnetic filling factor. This work opens new avenues for the use of high-magnetic-filling-factor cavities to achieve the strong-coupling regime with greater collective spin coupling than previously observed and with a variety of spin qubits. The patented cavity design [19,20] can be engineered to yield an arbitrary spectrum of cavity modes and, in principle, can be designed in such a way that the bright-mode frequency corresponds to the zero-field splitting of the NV defect, which enables the use of superconducting cavities and qubits by virtue of the fact that an applied dc magnetic field is no longer required. It may also be designed to allow the application of large external magnetic fields which can be beneficial in terms of reducing spin-bath decoherence. Finally and more generally, the system represents a sensitive method for electron paramagnetic resonance studies in solids.

The authors wish to acknowledge that this work was supported by Australian Research Council Grant No. CE110001013 and a University of Western Australia Research Collaboration Award. We also thank B. Johnson and T. Ohshima at JAEA for the diamond irradiation.

[1] K. Jensen, N. Leefer, A. Jarmola, Y. Dumeige, V. M. Acosta, P. Kehayias, B. Patton, and D. Budker, Phys. Rev. Lett. **112**, 160802 (2014).

[2] Y. Kubo, I. Diniz, C. Grezes, T. Umeda, J. Isoya, H. Sumiya, T. Yamamoto, H. Abe, S. Onoda, T. Ohshima, V. Jacques, A. Dréau, J.-F. Roch, A. Auffeves, D. Vion, D. Esteve, and P. Bertet, Phys. Rev. B **86**, 064514 (2012).

[3] A. Wallraff, D. I. Schuster, A. Blais, L. Frunzio, R.-S. Huang, J. Majer, S. Kumar, S. M. Girvin, and R. J. Schoelkopf, Nature (London) **431**, 162 (2004).

[4] Y. Kubo, F. R. Ong, P. Bertet, D. Vion, V. Jacques, D. Zheng, A. Dréau, J.-F. Roch, A. Auffeves, F. Jelezko, J. Wrachtrup, M. F. Barthe, P. Bergonzo, and D. Esteve, Phys. Rev. Lett. **105**, 140502 (2010).

[5] D. I. Schuster, A. P. Sears, E. Ginossar, L. DiCarlo, L. Frunzio, J. J. L. Morton, H. Wu, G. A. D. Briggs, B. B. Buckley, D. D. Awschalom, and R. J. Schoelkopf, Phys. Rev. Lett. **105**, 140501 (2010).

[6] V. Ranjan, G. de Lange, R. Schutjens, T. Debelhoir, J. P. Groen, D. Szombati, D. J. Thoen, T. M. Klapwijk, R. Hanson, and L. DiCarlo, Phys. Rev. Lett. **110**, 067004 (2013).

[7] X. Zhu, S. Saito, A. Kemp, K. Kakuyanagi, S.-i. Karimoto, H. Nakano, W. J. Munro, Y. Tokura, M. S. Everitt, K. Nemoto, M. Kasu, N. Mizuochi, and K. Semba, Nature (London) **478**, 221 (2011).

[8] R. Amsüss, C. Koller, T. Nöbauer, S. Putz, S. Rotter, K. Sandner, S. Schneider, M. Schramböck, G. Steinhauser, H. Ritsch, J. Schmiedmayer, and J. Majer, Phys. Rev. Lett. **107**, 060502 (2011).

[9] P. Bushev, A. K. Feofanov, H. Rotzinger, I. Protopopov, J. H. Cole, C. M. Wilson, G. Fischer, A. Lukashenko, and A. V. Ustinov, Phys. Rev. B **84**, 060501 (2011).

[10] S. Probst, A. Tkalčec, H. Rotzinger, D. Rieger, J. M. Le Floch, M. Goryachev, M. E. Tobar, A. V. Ustinov, and P. A. Bushev, Phys. Rev. B **90**, 100404 (2014).

[11] H. Paik, D. I. Schuster, L. S. Bishop, G. Kirchmair, G. Catelani, A. P. Sears, B. R. Johnson, M. J. Reagor, L. Frunzio, L. I. Glazman, S. M. Girvin, M. H. Devoret, and R. J. Schoelkopf, Phys. Rev. Lett. **107**, 240501 (2011).

[12] E. Abe, H. Wu, A. Ardavan, and J. J. L. Morton, Appl. Phys. Lett. **98**, 251108 (2011).

[13] G. Boero, G. Gualco, R. Lisowski, J. Anders, D. Suter, and J. Brugger, J. Magn. Reson. **231**, 133 (2013).

[14] J. H. N. Loubser and J. A. van Wyk, Rep. Prog. Phys. **41**, 1201 (1978).
[15] N. Bar-Gill, L. Pham, A. Jarmola, D. Budker, and R. Walsworth, Nat. Commun. **4**, 1743 (2013).
[16] C. Belthangady, N. Bar-Gill, L. M. Pham, K. Arai, D. Le Sage, P. Cappellaro, and R. L. Walsworth, Phys. Rev. Lett. **110**, 157601 (2013).
[17] R. Hanson, F. M. Mendoza, R. J. Epstein, and D. D. Awschalom, Phys. Rev. Lett. **97**, 087601 (2006).
[18] M. Goryachev, W. G. Farr, D. L. Creedon, Y. Fan, M. Kostylev, and M. E. Tobar, Phys. Rev. Appl. **2**, 054002 (2014).
[19] M. Goryachev and M. Tobar, Australia Patent No. AU2014903143 (12 August 2014).
[20] M. Goryachev and M. E. Tobar, New J. Phys. **17**, 023003 (2015).
[21] W. G. Farr, D. L. Creedon, M. Goryachev, K. Benmessai, and M. E. Tobar, Phys. Rev. B **88**, 224426 (2013).
[22] M. Goryachev, W. G. Farr, D. L. Creedon, and M. E. Tobar, Phys. Rev. A **89**, 013810 (2014).
[23] M. Goryachev, W. G. Farr, D. L. Creedon, and M. E. Tobar, Phys. Rev. B **89**, 224407 (2014).
[24] K. Benmessai, W. Farr, D. Creedon, Y. Reshitnyk, J.-M. L. Floch, T. Duty, and M. Tobar, Phys. Rev. B **87**, 094412 (2013).
[25] J.-M. L. Floch, R. Bara, J. G. Hartnett, M. E. Tobar, D. Mouneyrac, D. Passerieux, D. Cros, J. Krupka, P. Goy, and S. Caroopen, J. Appl. Phys. **109**, 094103 (2011).
[26] M. Hebbache, Phys. Rev. B **84**, 193204 (2011).
[27] E. van Oort, P. Stroomer, and M. Glasbeek, Phys. Rev. B **42**, 8605 (1990).
[28] C. Kollmar and H. Sixl, Mol. Phys. **45**, 1199 (1982).
[29] M. Hebbache, Phys. Rev. B **86**, 195316 (2012).
[30] S. Takahashi, R. Hanson, J. van Tol, M. S. Sherwin, and D. D. Awschalom, Phys. Rev. Lett. **101**, 047601 (2008).
[31] W. V. Smith, P. P. Sorokin, I. L. Gelles, and G. J. Lasher, Phys. Rev. **115**, 1546 (1959).